Supporting Information

Tumor microenvironment-responsive nanoplatform based on biodegradable liposome-coated hollow MnO_2 for synergistically enhanced chemotherapy and photodynamic therapy

Xiangtian Deng [1, 2], Qingcheng Song [2], Yiran Zhang[1,2], Weijian Liu[3, #], Hongzhi Hu[3, #], Yingze Zhang[1, 2, #]

[1] School of Medicine, Nankai University, Tianjin, 300071, China

[2] Department of Orthopaedic Surgery, The Third Hospital of Hebei Medical University, Shijazhuang, 050051, China.

[3] Department of Orthopaedics, Union Hospital, Tongji Medical College, Huazhong University of Science and Technology, Wuhan 430022, China.

Disclosure statement

There are no conflicts of interest to declare.

Authors contributions

Xiangtian Deng wrote the manuscript. Qingcheng Song and Yiran Zhang was responsible for language modification and correction. Professor Weijian Liu, Professor Hongzhi Hu, and Professor Yingze Zhang illuminated instruction and expert advice for this paper.

Corresponding author

[#] Correspondence to Weijian Liu, Hongzhi Hu, and Yingze Zhang.

E-mail: zyz050051@163.com

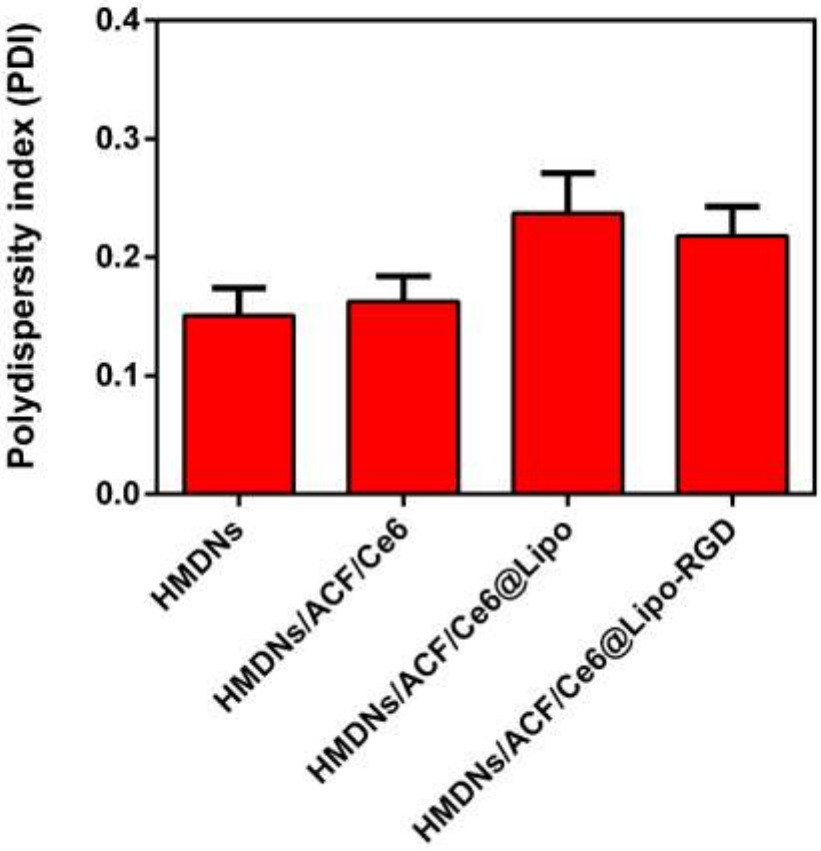

Figure S1. PDI values of HMDNs, HMDNs/ACF/Ce6, HMDNs@Lipo, and HMDNs@Lipo-RGD determined by DLS (mean ± SD, n=3).

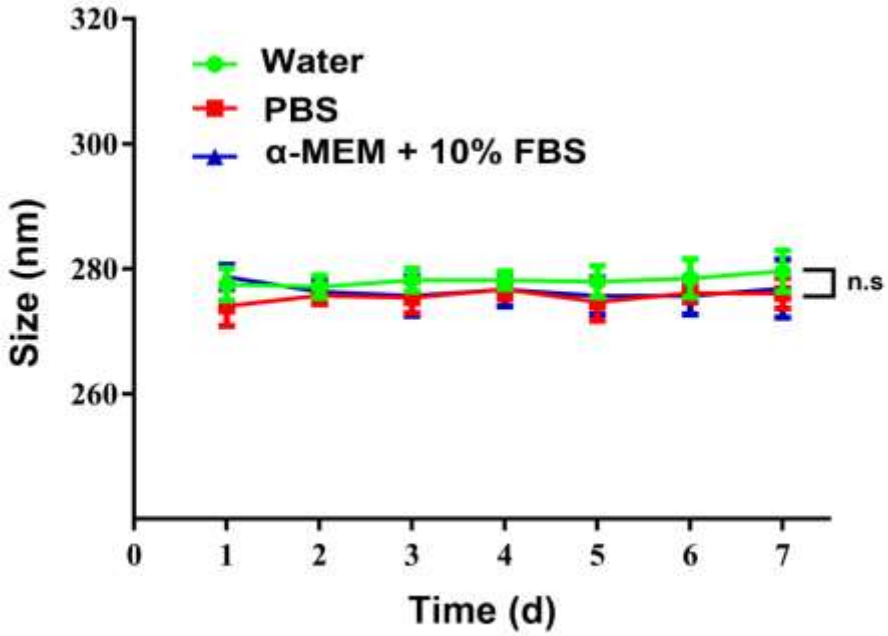

Figure S2. Size distribution of HMDNs/ACF/Ce6@Lipo-RGD NPs for 7 days. n.s indicated not significant.

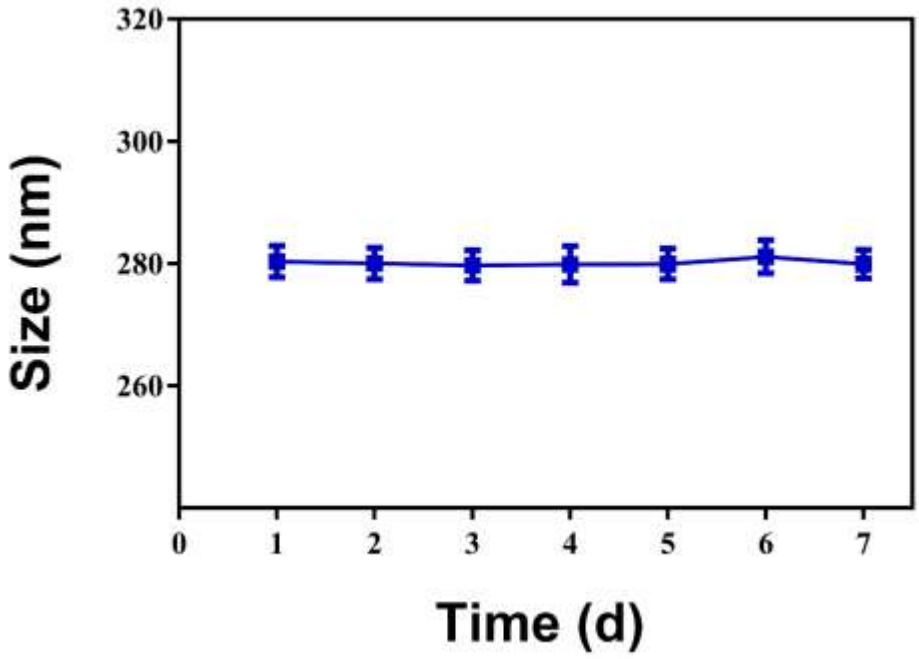

Figure S3. Changes in particle size of nanoparticle during plasma stability assay for 7 days.

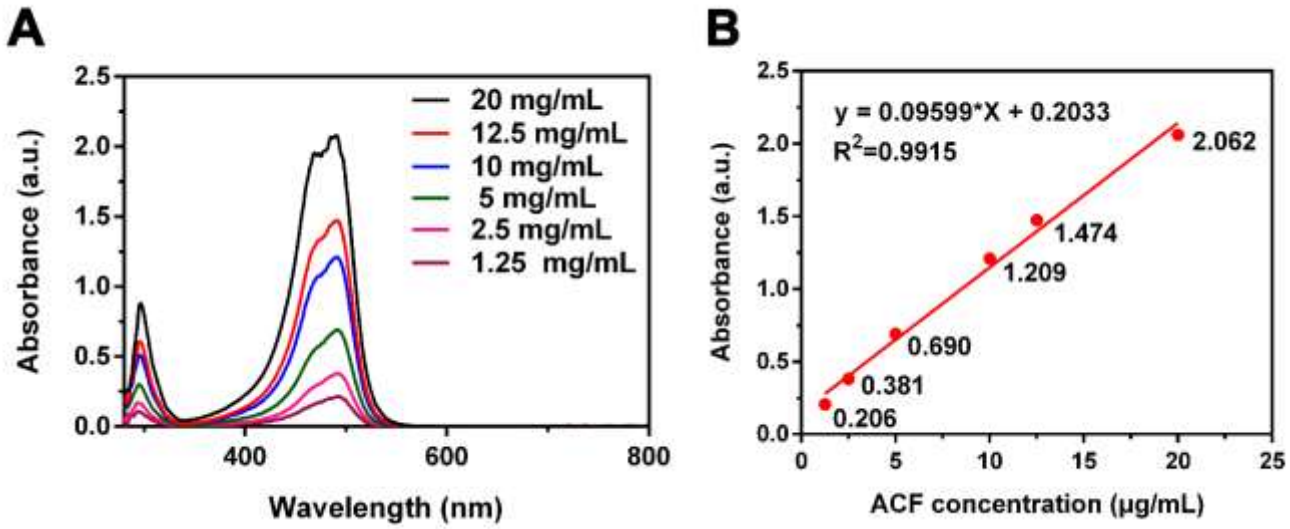

Figure S4. (**A)** The absorption spectra of ACF with different concentrations. (**B)** The standard curve of ACF determined by a UV-VIS spectrophotometer.

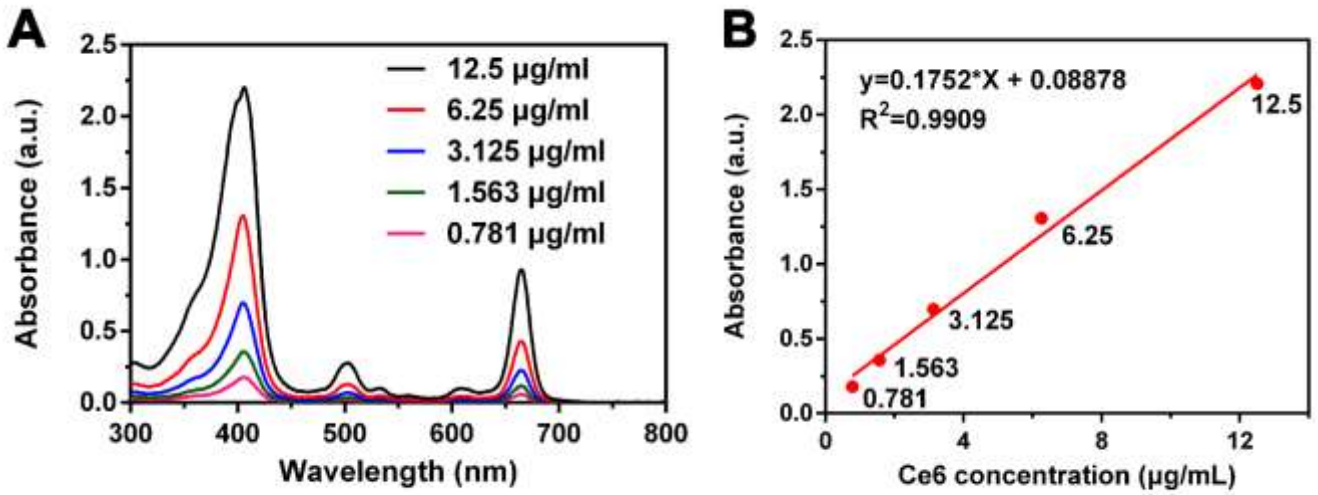

Figure S5. (**A)** The absorption spectra of Ce6 with different concentrations. (**B)** The standard curve of Ce6 determined by a UV-VIS spectrophotometer.

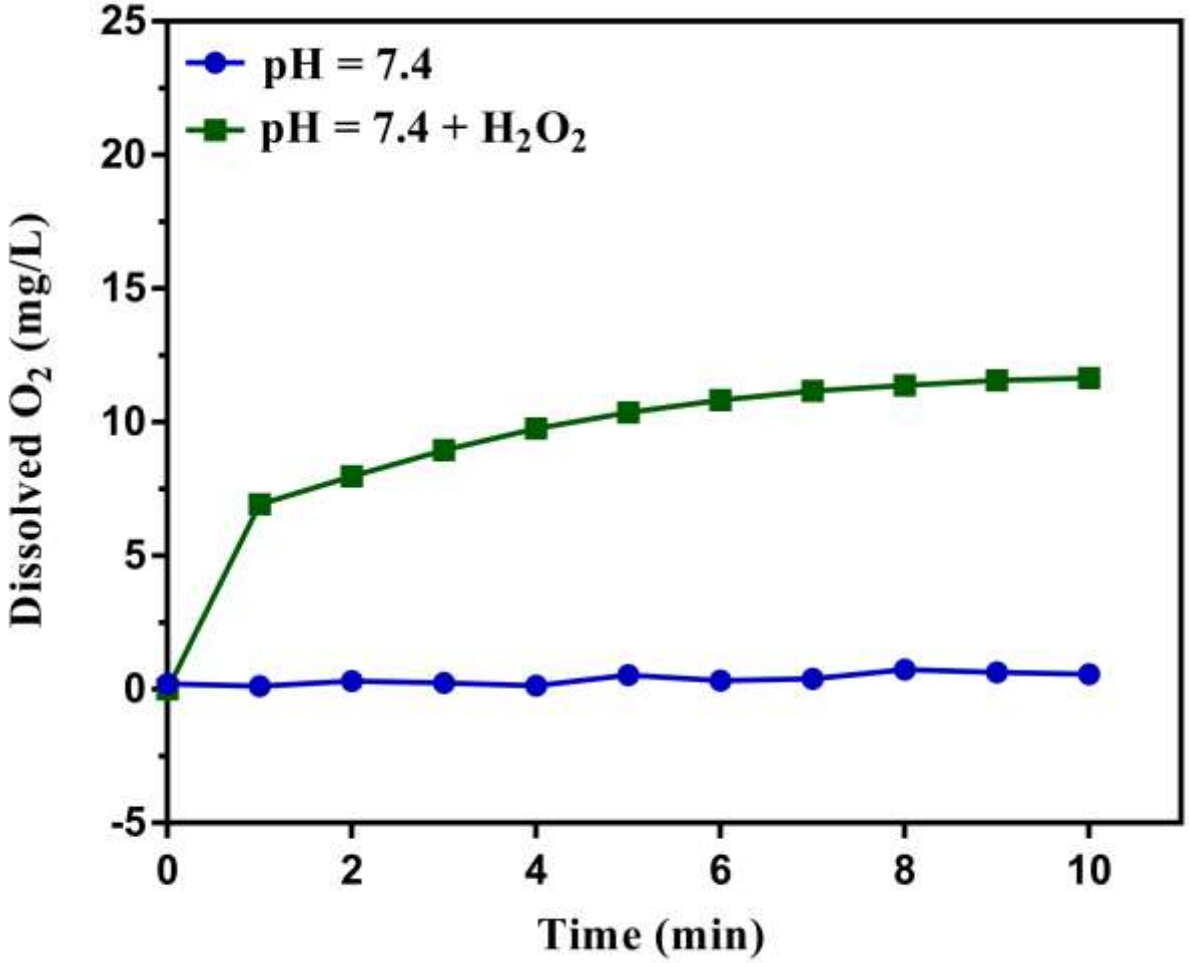

Figure S6 Detection of O_2 generation from HMDNs@Lipo-RGD NPs determined by a portable dissolved oxygen analyzer at pH 7.4 in the presence or absence of H_2O_2 solutions.

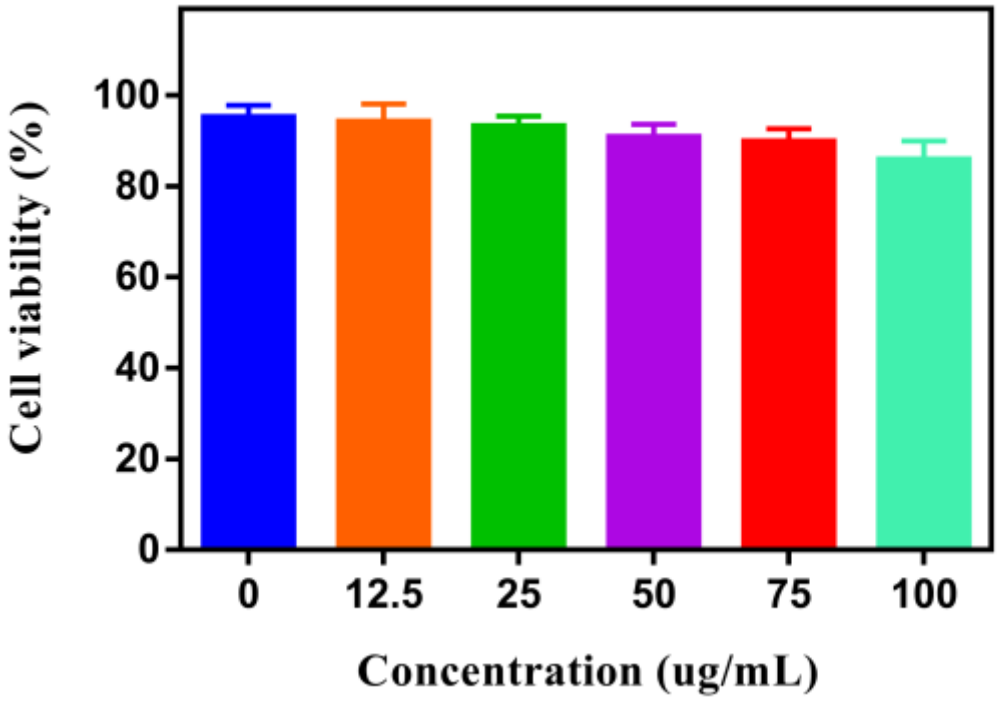

Figure S7. Cell viability of MNNG/HOS cells treated with different concentration of HMDNs@Lipo-RGD.

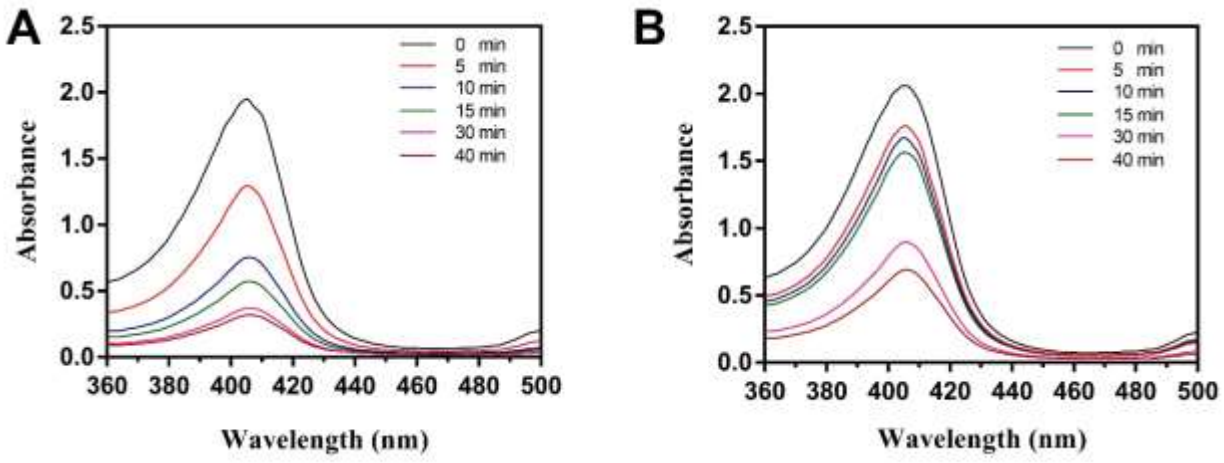

Figure S8. Time-dependent absorbance changed caused by 660 nm light irradiation. **(A)** free Ce6; **(B)** HMDNs/Ce6@Lipo-RGD nanoparticle.

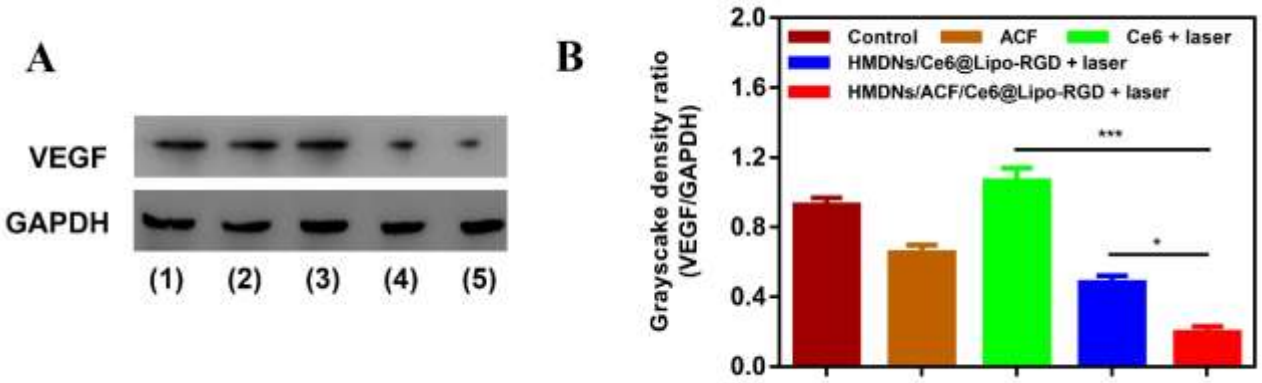

Figure S9 (A) Western blotting analysis of VEGF expression in MNNG/HOS cells after corresponding treatment (Groups included (1) control, (2) Free ACF, (3) Ce6+ laser, (4) HMDNs/Ce6@Lipo-RGD + laser, and (5) HMDNs/ACF/Ce6@Lipo-RGD + laser). (**B)** VEGF levels were determined by grayscale density value.

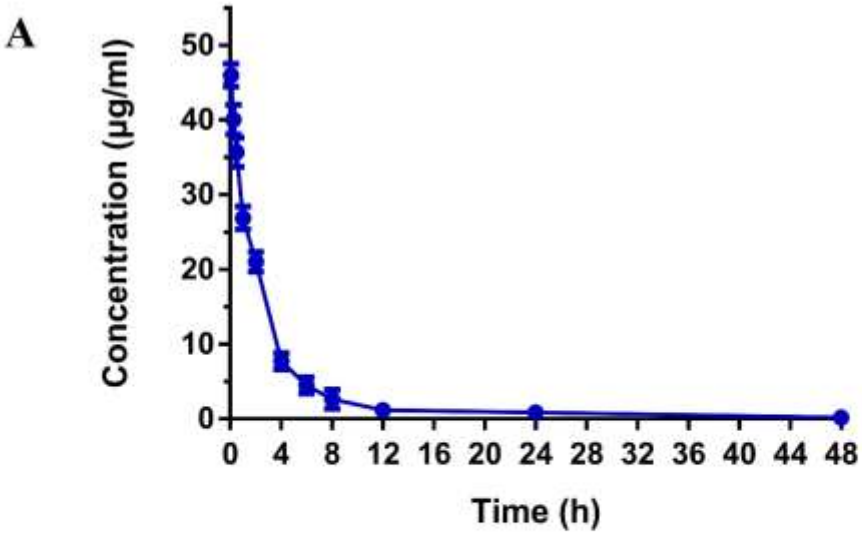

B

Paramaters	$AUC_{0\text{-}48h}$ (μg · h/mL)	MRT (h)	t1/2 (h)
HMDNs@Lipo-RGD	137.6	7.87	6.13

Figure S10 The profiles of HMDNs@Lipo-RGD NPs concentration-time (A) and (B) pharmacokinetic parameters after intravenous injection in BALB/c mice (n=3).

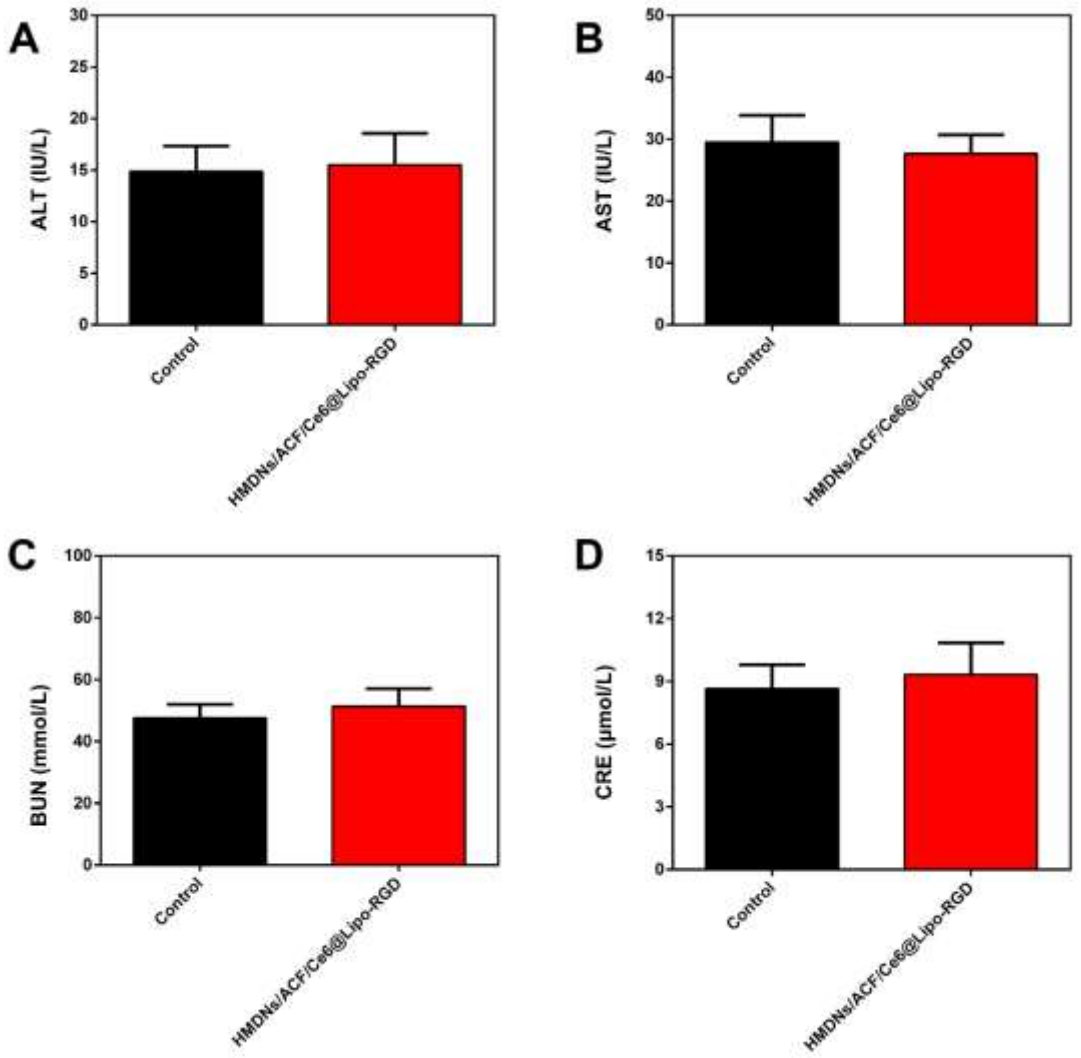

Figure S11. Biosafety evaluation by serum biochemistry analysis. (**A-B)** Serum levels of liver function markers, ALT and AST. (**C-D**) Serum levels of kidney function markers, BUN and CRE.